

AD656876

RECEIVED  
AUG 21 1967

## Interstitial Pulmonary Edema

### An Electron Microscopic Study of the Pathology of Staphylococcal Enterotoxemia in Rhesus Monkeys

Milton J. Finegold, M.D.

The toxicity of staphylococcal enterotoxin B for humans and experimental animals has been investigated for several years without definitive understanding of the mechanism of its action.<sup>23</sup> In some of these studies, including autopsies on two children who died after ingestion of enterotoxin in contaminated goat's milk,<sup>24</sup> the most significant pathologic finding has been pulmonary edema. Systemic administration of the toxin in monkeys was said to produce lethal pulmonary edema,<sup>11</sup> as did the accidental instillation of toxin into the trachea of a monkey during a study of the gastrointestinal pathology.<sup>8</sup> A recent investigation of the clearance of isotopically labeled enterotoxin following intravenous administration revealed the accumulation of toxin in the lungs of monkeys.<sup>5</sup> There have been no publications on the pulmonary pathology of experimental enterotoxemia. A report of the light and electron microscopic findings in rhesus monkeys given staphylococcal enterotoxin B intravenously is presented.

#### METHODS\*

Rhesus monkeys obtained from commercial sources were housed locally for at least 90 days before use. Young animals of both sexes weighing 2 to 4 kg. each had

Accepted for publication March 1, 1967.

From the Medical Sciences Laboratory, Department of the Army, Fort Detrick, Frederick, Maryland.

\*In conducting the research reported herein, the investigator adhered to "Guide for Laboratory Animal Facilities and Care" established by the Committee on a Guide for Laboratory Animal Facilities and Care of the Institute of Laboratory Animal Resources, National Academy of Sciences-National Research Council.

no known prior experience with enterotoxin, nor were they used in any other experiment. Purified staphylococcal enterotoxin B, in the form of a dry powder,<sup>18</sup> was dissolved in pyrogen-free normal saline. Between 8:30 and 10:00 a.m., each monkey received a single rapid intravenous injection of 0.1 to 1.0 ml. containing from 15 to 300  $\mu$ g. of toxin per kg. of body weight.\* The monkeys were observed every 4 hours and were sacrificed with intravenous sodium pentobarbital when moribund. In addition, randomly selected animals were sacrificed at 1, 3, 6, 12, 24, 48, 72, 96, and 120 hours. The lungs were excised, freed of mediastinal tissues, and weighed. They were fixed by endotracheal perfusion with 2 per cent glutaraldehyde buffered to pH 7.2 by 0.1 M phosphate to give a total osmolality of 444 mOsmoles. The perfused lungs were immersed in the same fluid at 0-4° C. for 1 hour, then sectioned. Three to 10 1-mm. cubes of tissue from representative areas of each lung were taken for electron microscopic examination and 1- by 1- by 0.3-cm. sections of all lobes were excised for paraffin embedding and light microscopic study. Further processing for electron microscopy consisted of washing in buffer adjusted to 444 mOsmoles with 0.25 M sucrose, mincing in buffer, postfixing in osmium tetroxide for 1 hour, dehydrating in alcohol, embedding in Epon 812, sectioning with a Porter-Blum MT-1 microtome, treating sections on unsupported grids with a saturated solution of uranyl acetate, and examining in an RCA EMU 3-G microscope.

Routine sections of heart, lymph nodes, liver, spleen, stomach, jejunum, ileum, colon, kidney, and brain were taken from

selected animals for light microscopic examination.

### RESULTS

Each of 32 rhesus monkeys was given one intravenous injection of enterotoxin in a dose of 15, 20, 100, or 300  $\mu$ g. per kg. of body weight. These doses were intermediate between a previously established effective dose<sub>50</sub>, 1  $\mu$ g. per kg. as measured by vomiting,<sup>18</sup> and a lethal dose<sub>75</sub>, 1 mg. per kg.<sup>19</sup> There was considerable variation in each group with maximal effect, in terms of pulmonary edema, obtained at 20  $\mu$ g. per kg. At each dose level animals remained alert and active, despite an initial episode of vomiting and a persistent mild diarrhea, until 40 to 48 hours. At that time some monkeys refused food and became lethargic, with slow and deep respiration, progressing to stupor at the time of sacrifice between 45 and 55 hours. Animals failing to show these signs by

48 hours invariably remained well and had no evidence of pulmonary edema when sacrificed.

The presence and degree of edema were measured by an index of lung weight to body weight. Body weights ranged from 1.94 to 3.44 kg., and lung weights varied from 16 to 55 gm. The index ranged from 6.0 to 23. A value of 10 was established as the upper limit of normal, as determined by numerous controls and confirmed by correlation with the light microscopic findings. Twelve monkeys were sacrificed prior to 48 hours, with no clinical evidence of illness other than diarrhea. All had indices below 10, and no pulmonary pathology was found by light or electron microscopy.

Among the remaining 20 monkeys, only eight had an index above 10. In each of these eight, the index correlated with the degree of pulmonary edema seen with the light microscope and with the presence of

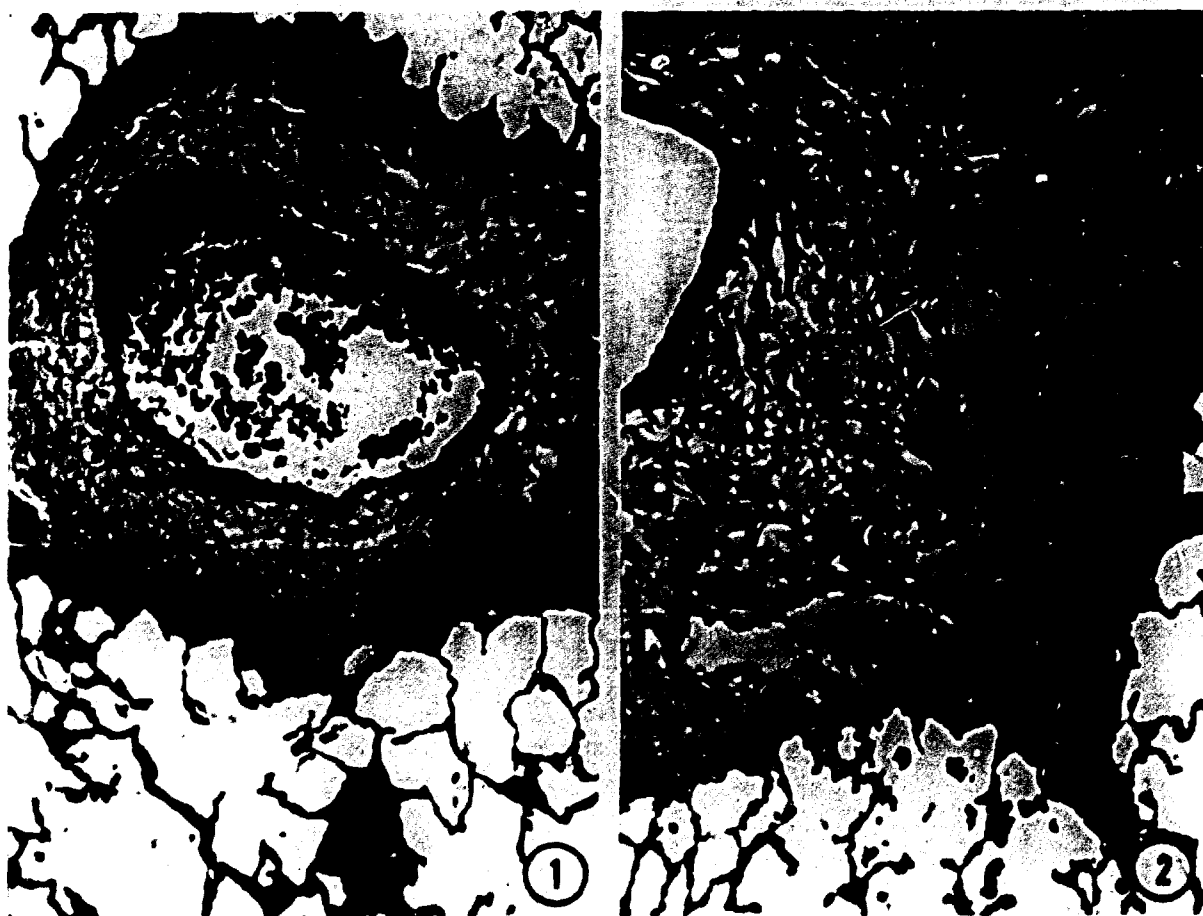


FIG. 1. A pulmonary vein (*above*) and arteriole (*below*) are surrounded by edematous interstitial tissue.  $\times 65$ .

FIG. 2. A pulmonary vein lies to the *upper left*. The adjacent connective tissue is edematous. Large, dilated lymphatics are seen to the *right*.  $\times 65$ .

lesions found in the electron microscopic examination. A detailed description of the findings in these eight monkeys follows.

### LIGHT MICROSCOPY

*Lungs.* Marked perivascular interstitial edema was present in all lobes (Figs. 1 and 2). In these areas lymphatic vessels were distended by large quantities of amorphous eosinophilic fluid, occasionally containing red blood cells. Smaller venules were frequently distended with blood cells, yet alveolar capillaries were not significantly congested. There were few scattered foci of intraalveolar edema (Fig. 3), in which the fluid had often been condensed artifactually in processing into coarse granular and fibrillar eosinophilic matter. Some alveoli and the septa in such foci contained an excess of mononuclear cells, including finely vacuolated pulmonary histiocytes and plump monocytes without lipid vacuoles, and a few lymphocytes and neutro-

philic granulocytes (Fig. 4). Lesions of capillary and venule endothelium could not be discerned in either standard 5- $\mu$  paraffin-embedded sections or in 1- $\mu$  plastic-embedded sections at magnifications up to  $\times 1250$ .

*Gastrointestinal Tract.* Stomach, jejunum, ileum, and descending colon were examined. There were no significant differences among the eight monkeys dying 45 to 55 hours after enterotoxin and numerous control animals from other experiments.

*Other Organs.* There were no consistent or significant findings in lymph nodes, heart, spleen, liver, kidney, or brain.

### ELECTRON MICROSCOPY

Examination was limited to the lungs.

*Venules.* Most of the venules examined showed only an accumulation of slightly granular, electron-opaque fluid in the adventitia, with focal separation of collagen, smooth muscle, and elastic tissue of the

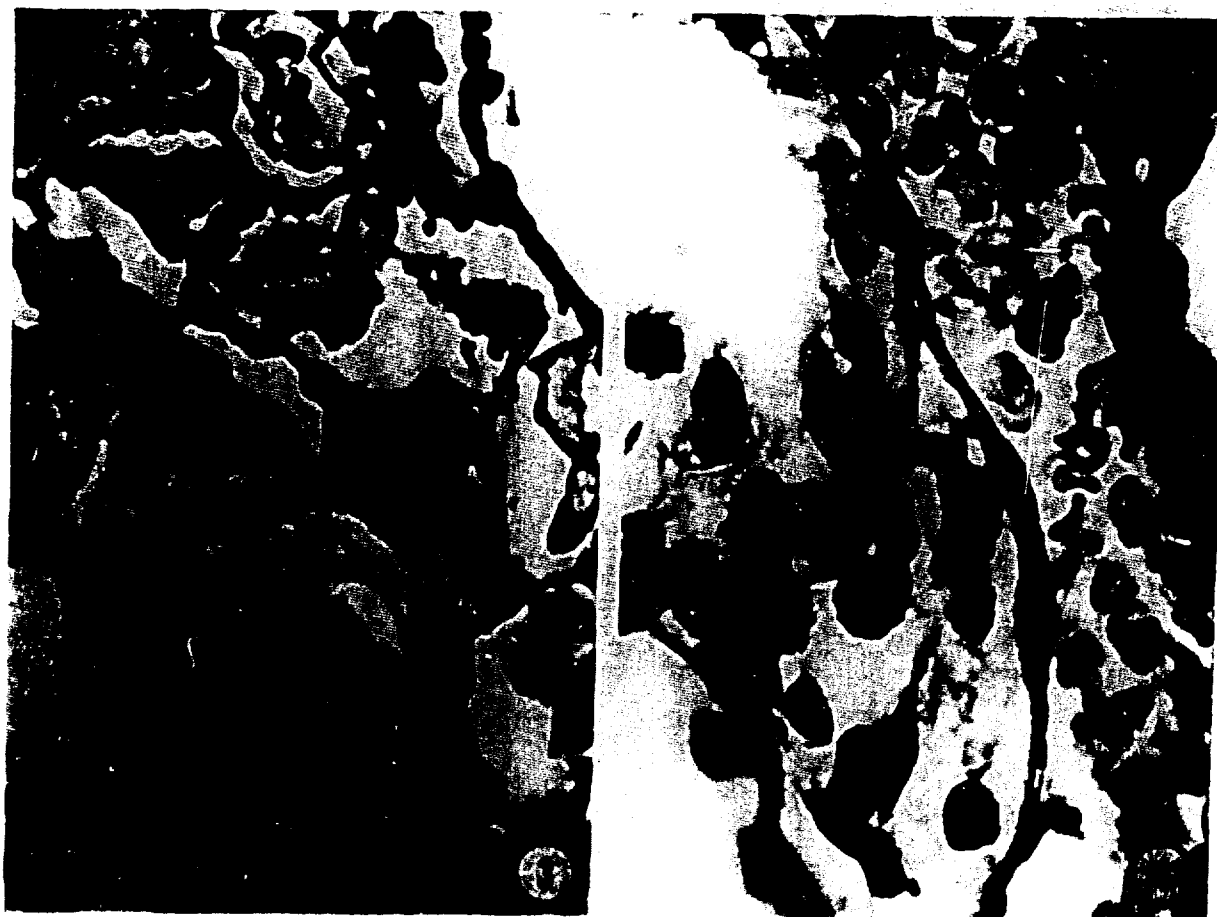


FIG. 3. Alveoli contain edema fluid, some of which is coarsely granular or fibrillar. A few mononuclear cells are found in septa and alveoli.  $\times 200$ .

FIG. 4. The interstitium adjacent to a venule is crowded with mononuclear cells. Small lipid droplets fill the cytoplasm of two such cells on the left.  $\times 650$ .

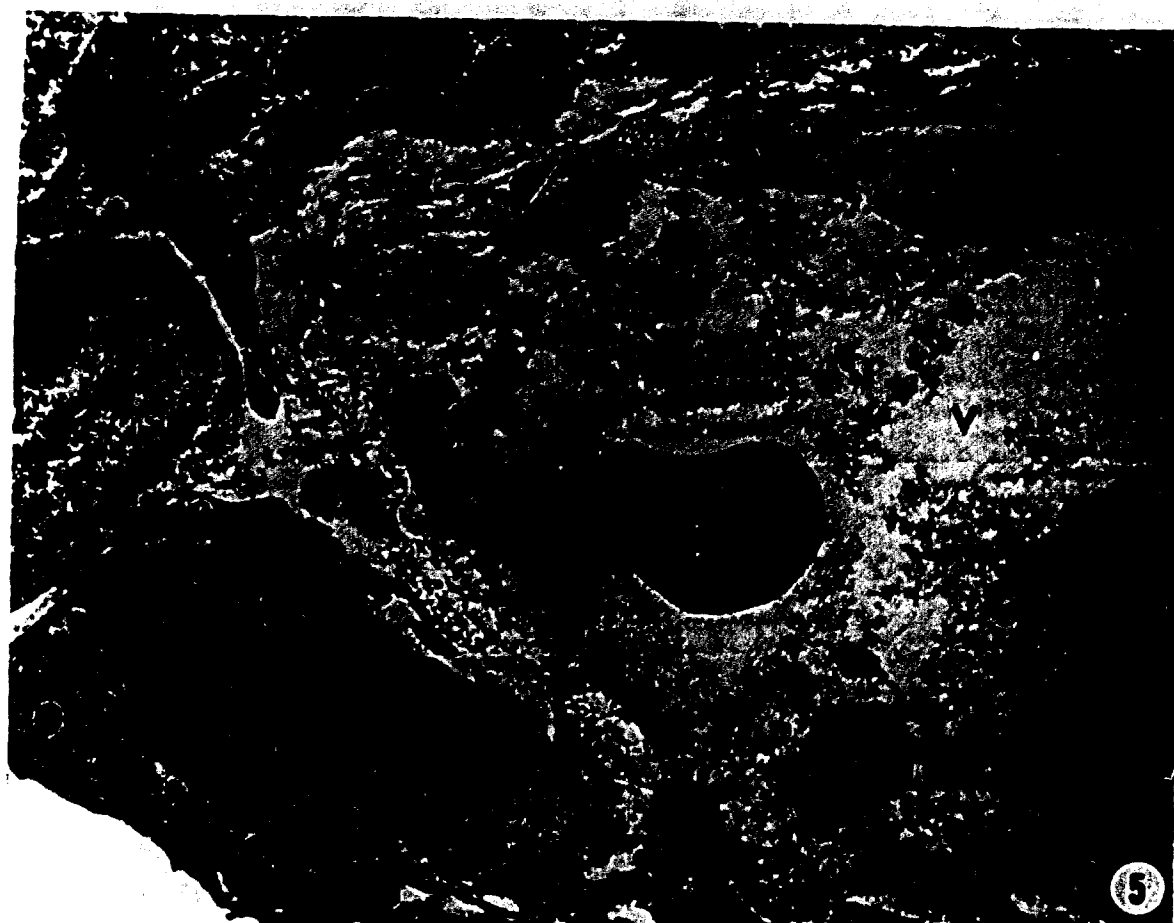


FIG. 5. A venule with lumen (V) containing a red blood cell (dark homogeneous body, center). There are foci of endothelial degeneration with discontinuity of the surface (arrows). A histiocyte is at lower left and two alveolar septal cells are at mid- and upper left.  $\times 50000$ .

tunica media by the fluid but no endothelial lesions. However, an occasional venule displayed focal endothelial cell disruption with discontinuity of the lining and electron-dense or granular alteration of endothelial cell cytoplasm (Fig. 5, arrows). Adventitial edema was continuous with the excess fluid in the interstitium, and red blood cells were commonly found in these extravascular locations (Fig. 6). Occasionally, mast cells were found in the walls of veins and venules; they were not degranulated or otherwise remarkable.

**Capillaries.** The most striking, numerous, and diverse lesions involved capillary endothelial cells. Complete cell *necrosis* was defined as fragmentation of cell constituents with interruption of the plasma membrane, increased electron opacity, dense granularity, and swelling (Fig. 7). *Degenerative* changes were defined as increased density and granularity of the cytoplasm (Fig. 8), marked swelling of the

cytoplasm with rarefaction and dispersion of organelles (Fig. 9), or swelling with increased size and numbers of vacuoles in the cytoplasm (Fig. 10). Thus, necrosis is considered an extension and combination of the degenerative changes. In each example, it may be noted that the necrotic or degenerated cells retained continuity with entirely normal endothelial cells.

Crystalloids were encountered occasionally in pulmonary capillaries from both control and experimental animals. Within one swollen and granular capillary endothelial cell (Fig. 11), such a crystalloid remained intact in the cytoplasm. The structure shown measures approximately 800 by 360 m $\mu$  and consists of a lattice having equal periodicity of approximately 266 Å in both directions. As seen in another example from a normal monkey (Fig. 12), there may be some relationship to microtubules at the periphery of the lattice. Another form of crystal has been de-

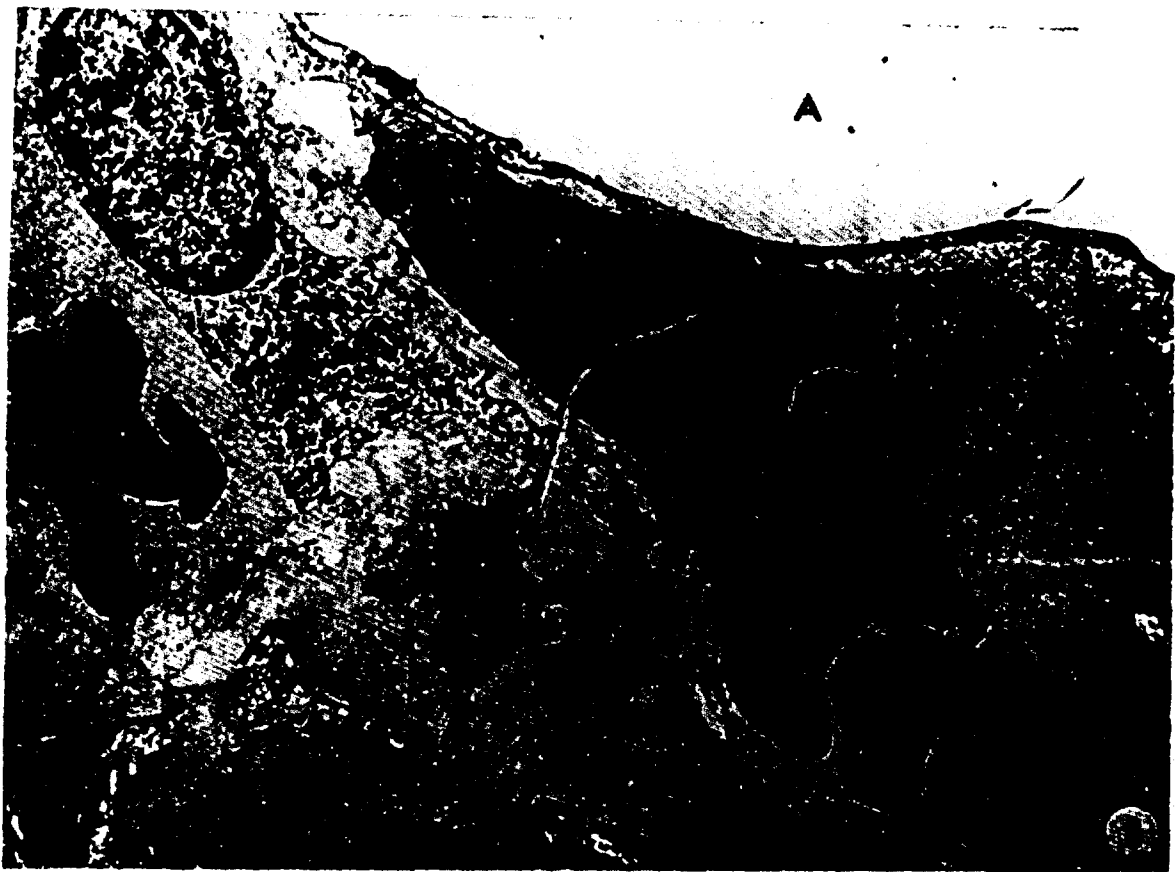


FIG. 6. Interstitial edema and hemorrhage (*I*). The alveolar lumen (*A*) is at upper right. Portions of several septal cells, smooth muscle cells (*below, left*), and bundles of collagen and elastic tissue are spread apart by fluid containing erythrocytes (*I*).  $\times 5000$ .

scribed in the endothelium of arteries.<sup>30</sup> Some cytoplasmic bodies within otherwise intact endothelial cells were found in the experimental series only, and they appear to represent phagocytosed material, of either extraneous or intracellular origin (Figs. 13 to 15). The round, homogeneous body on the left in the endothelial cell of Figure 13 has a single membrane and may qualify as a lysosome. Also in this section is an irregularly serrated inclusion of unknown type in the interstitial tissue between the epithelial and endothelial cell basement membranes (*upper arrow*). Such a separation of basement membranes in the alveolar wall should not be attributed to interstitial edema, as it is a structural feature of normal lungs. Pinocytotic vesicles, which are evident in all photographs of capillary endothelia, were not detectably more numerous in the edematous lungs.

One finding, restricted to edematous lungs, consisted of intracapillary hernia-

tion of endothelial cells (Figs. 16 to 18). Interstitial fluid, acting perhaps at a point of least resistance, accumulated under the attenuated segment of endothelial cell cytoplasm, causing it to be lifted off the basement membrane and to protrude into the capillary lumen. In Figure 17 it is possible to trace the normal endothelial cell plasma membranes as they curve upward in a hairpin turn (*narrow, right*) to form the large, fluid-filled bleb in the capillary lumen. On the lower left, the intact junction between the considerably thinned and stretched cell of the bleb and the adjacent normal endothelial cell is seen (*lower arrow*). Although the pressure of interstitial fluid produced a considerable herniation of the attenuated endothelial cell in Figure 18, there is no detectable spreading of the collagen bundles lying in direct continuity with this fluid in the upper left of the figure.

The endothelial bleb shown in Figure 16, although also enclosed by a very definite

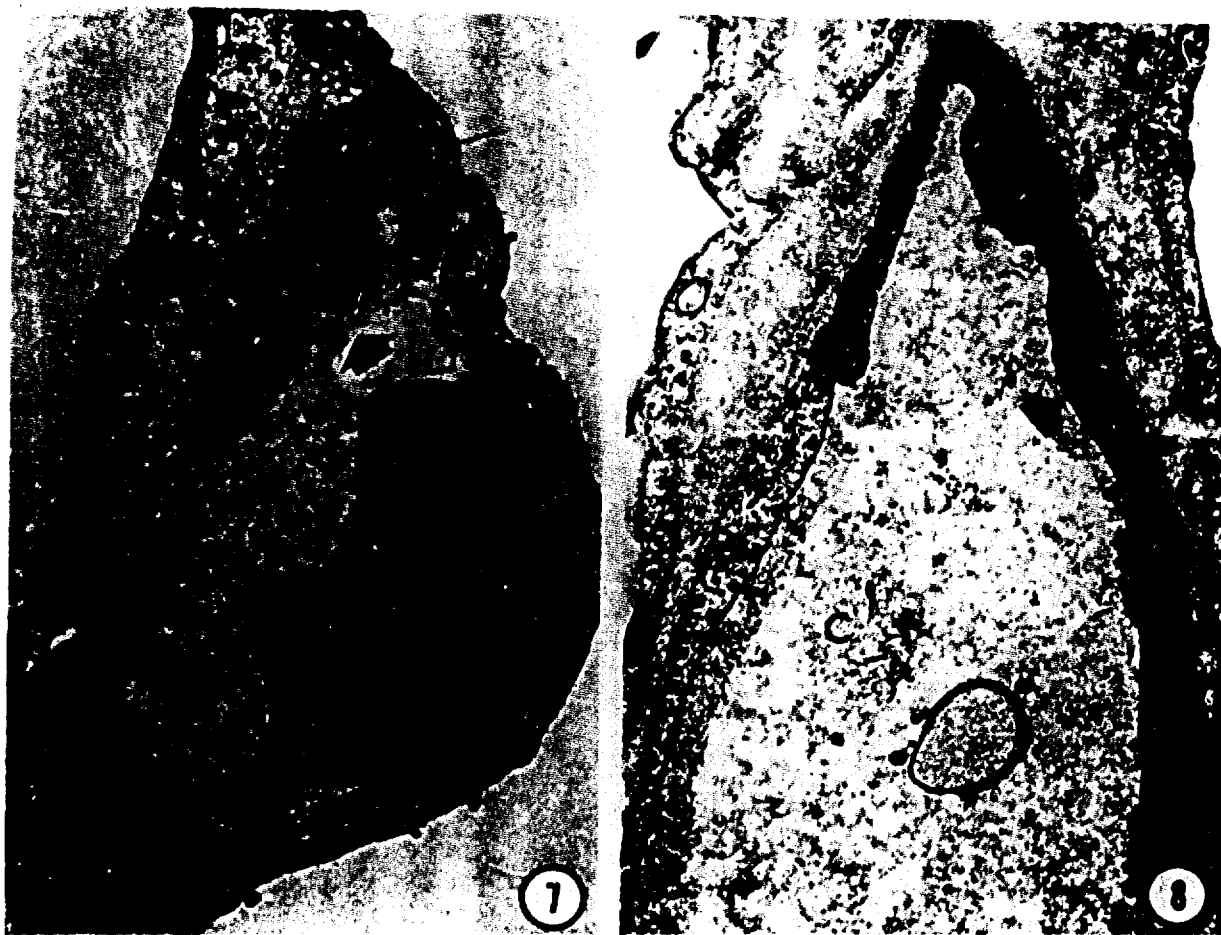


FIG. 7. Necrosis of capillary endothelium (*arrows*). The capillary lumen (*C*) contains a red blood cell. The thin endothelial segment *below* and to the *right* of the red blood cell is normal. Note the persistence of intact junctions between this cell and the granular, dense, swollen, and fragmented endothelial cells to the *left*.  $\times 10,000$ .

FIG. 8. Endothelial cell degeneration (*arrow*). Continuity persists between an intact endothelial cell (*left*) and one showing increased cytoplasmic opacity, dense bodies, and slightly enlarged vesicles (*right*).  $\times 20,000$ .

double row of plasma membranes to indicate lifting of an intact cell, differs from the following figures because of the presence of cellular debris within it, especially in the basal portion of the bleb adjacent to the basement membrane. This suggests that some damage to the nonluminal plasma membrane may have occurred to release that structure from its connective tissue attachments.

**Alveolar Epithelial Lining.** Very rarely, a portion of a thin squamous epithelial cell (type I alveolar lining cell<sup>2</sup>) was similarly raised from the basement membrane and protruded into the alveolar space, apparently impelled by the pressure of underlying interstitial fluid (Figs. 16 and 19). Again, the presence of some ill-defined debris along the epithelial basement mem-

brane (Fig. 16) suggests at least focal damage to the plasma membrane, perhaps in a different plane of sectioning, as the elevated epithelial cell membranes seem intact wherever they are sharply cut.

Actual separation of alveolar epithelium was seen in a few sections. Figure 20 shows such a gap measuring 280  $\mu$ . Extending through the space from basement membrane to alveolar lumen is dense fibrillar material that displays the 220- to 240-Å periodicity of fibrin<sup>12</sup> under higher magnification. Fibrin was sometimes found in the interstitium and was a conspicuous component of the meager alveolar exudate (Fig. 21).

There was no significant alteration of the granular pneumocytes (type II alveolar epithelial cell<sup>2</sup>) in any of the experimental animals.

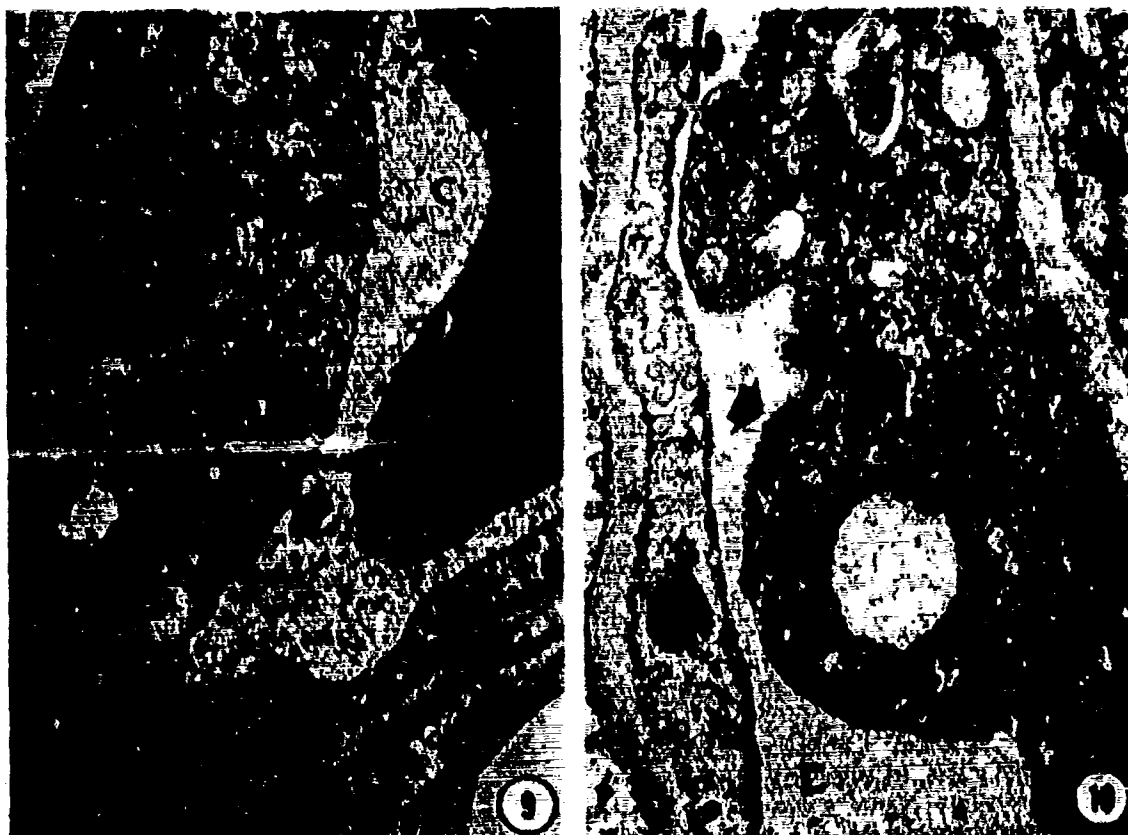


FIG. 9. Endothelial cell degeneration (*arrow*). There is rerefraction and swelling of the cytoplasm. Continuity with the unaffected cell (*right*) is maintained. C, Capillary lumen.  $\times 25,000$ .

FIG. 10. Endothelial cell degeneration (*arrow*). The swollen cell contains many vacuoles, bound by either single or double membranes.  $\times 25,000$ .

FIG. 11. Endothelial cell degeneration. A swollen, dense, and granular capillary endothelial cell contains a crystalloid (*arrow*) (see text, page 915). C, Capillary lumen.  $\times 25,000$ .

FIG. 12. Crystalloid from a normal monkey, pulmonary capillary endothelium (see text, page 915).  $\times 75,000$ .

FIG. 13. Cytoplasmic and interstitial inclusions. A capillary endothelial cell contains a lysosome (*lower left arrow*) and a second inclusion (*lower right arrow*). Above them in the interstitium between the epithelial and endothelial basement membranes (*bar*), there is another unidentified inclusion (*upper arrow*).  $\times 15,000$ .

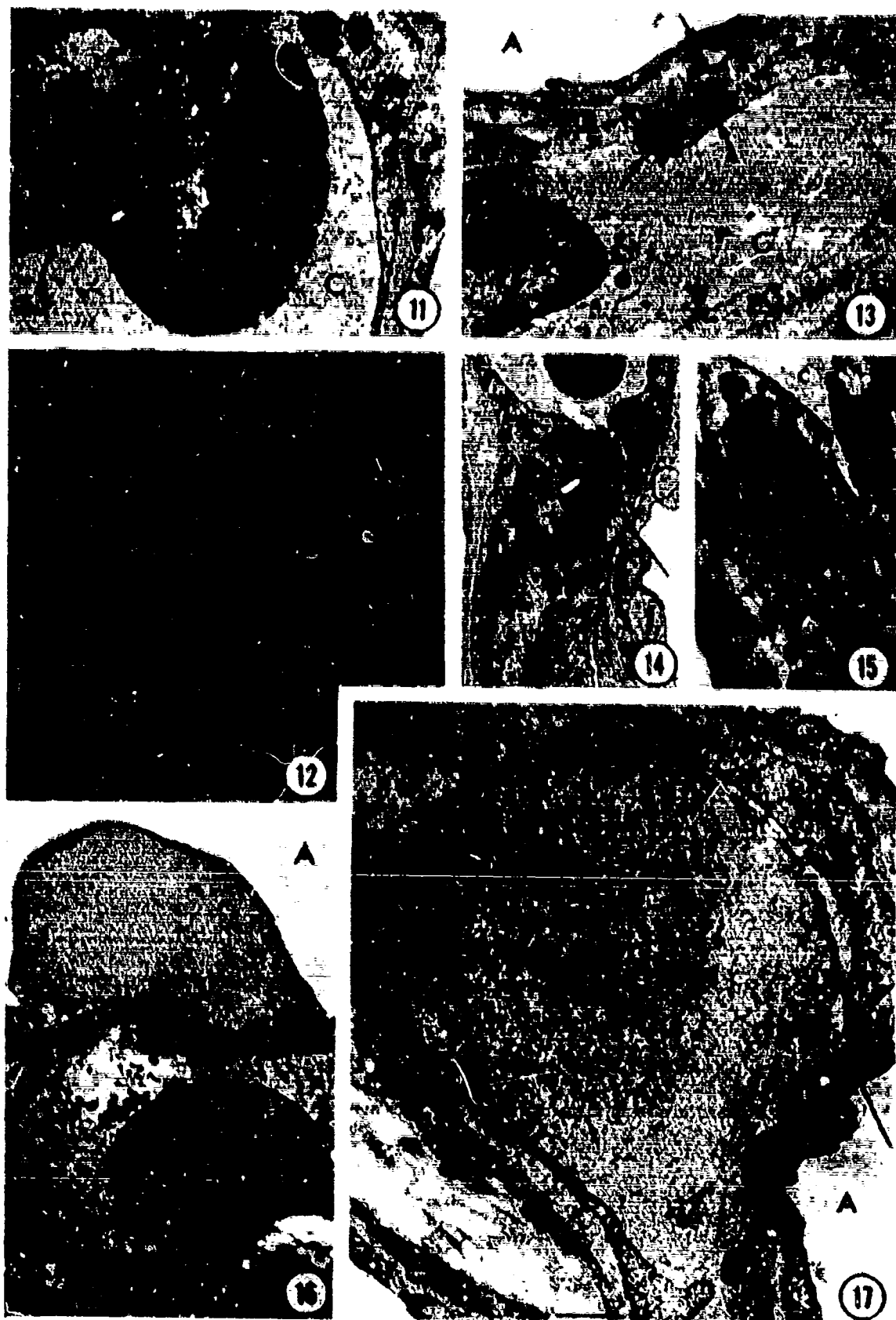
FIG. 14. Endothelial cell inclusions (*arrow*).  $\times 10,000$ .

FIG. 15. Endothelial cell inclusions. Within a protuberance of capillary endothelial cytoplasm lies an aggregate of dense, partly structured, and incompletely bound material.  $\times 25,000$ .

FIG. 16. Epithelial and endothelial blebs. Protruding into the alveolus (A), the epithelial cell is elevated by finely granular fluid. The plasma membranes appear intact where the sectioning is sharp. Within the bleb, lying on the basement membrane, is some debris. A similar appearance is provided by an endothelial cell, which is lifted into the capillary lumen (C) by fluid. The membranes again seem intact, although more cellular debris is noted.  $\times 15,000$ .

FIG. 17. Effects of edema. A large bleb of fluid produces herniation of the thin segments of endothelium into the lumen of a capillary (C). There is no question that the cell is intact since continuity of the redundant loop and remainder of the cell can be seen (*arrow, right*), as well as the junction with the adjacent endothelial cell (*arrow, bottom*). The plasma membranes are well defined and unremarkable. The epithelial basement membrane at the mouth of the sac may be traced, but the endothelial membrane is not detectable.  $\times 20,000$ .





FIGS. 11 to 17

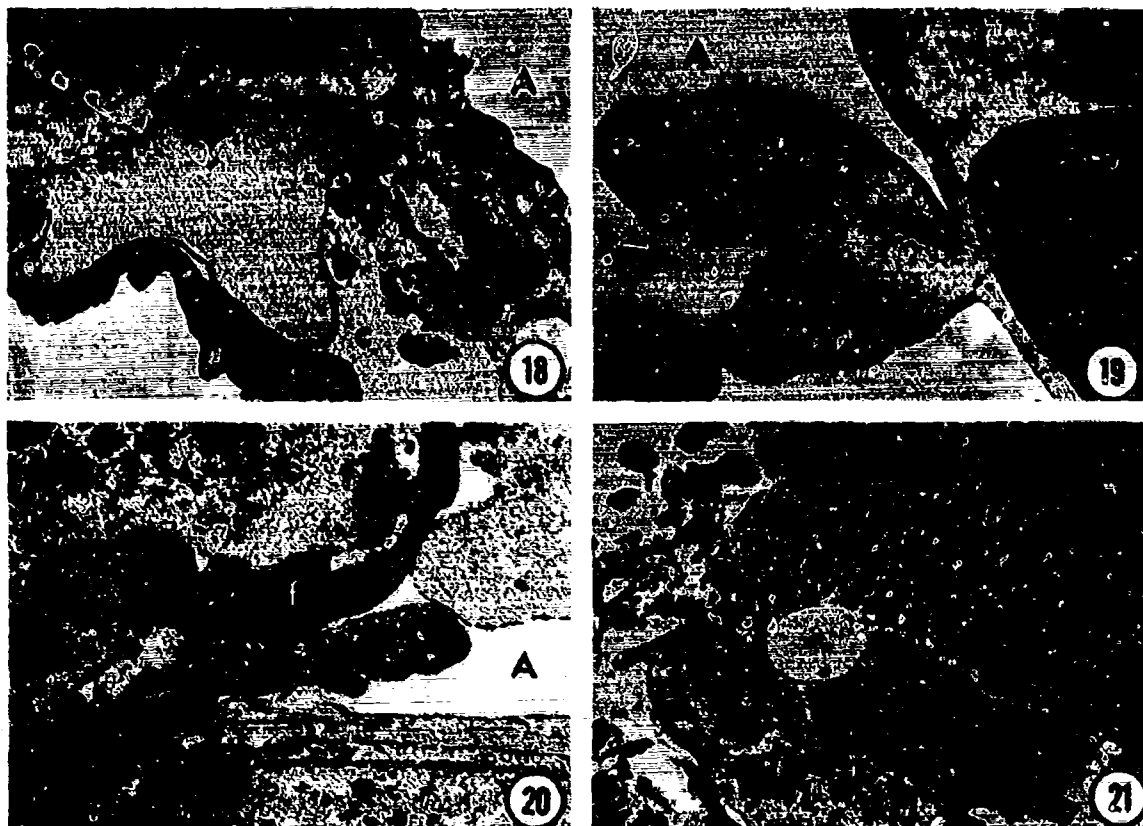


FIG. 18. Interstitial edema (*I*). The endothelial cell is herniated into the capillary lumen (*C*), but the collagen bundles at the *upper left* are not spread apart or otherwise abnormal. The remainder of the endothelial cell contains multiple cytoplasmic inclusions (*middle, right*). *A*, Alveolar lumen.  $\times 10,000$ .

FIG. 19. Epithelial cell herniation. The thin segment of a squamous cell is forced into the alveolar lumen (*A*) by the pressure of underlying edema fluid. The plasma membranes are intact and the basement membrane can be traced across the mouth of the hernia (*arrow*). To the right are two red blood cells in the interstitium (*I*) along with edema fluid.  $\times 15,000$ .

FIG. 20. Epithelial cell separation. A gap between the thin segments of squamous epithelial cells is filled by fibrin (*f*) that extends from basement membrane to alveolus (*A*), where it is surrounded by portions of a macrophage. The basement membrane appears intact.  $\times 25,000$ .

FIG. 21. Alveolar exudate. A macrophage (*M*) has abundant fibrin (*f*) within the grasp of its pseudopods. Cell debris is also present.  $\times 7,500$ .

**Alveolar Septa.** The focal inflammatory reaction observed with the light microscope consisted predominantly of cells derived from blood monocytes.<sup>3</sup> *Monocytes* were common within capillaries (Fig. 22), *histiocytes* were numerous in the interstitium (Fig. 5), and *macrophages* were found in the alveoli (Fig. 21). The cells acquired abundant rough-surfaced endoplasmic reticulum, lipid droplets, autophagic vacuoles, and lysosomes in their passage from circulation to airway, and some histiocytes were seen to divide. An early stage in the migration of a monocyte into the inter-

stitium through a gap in capillary endothelium is shown in Figure 22. This defect is also associated with interstitial hemorrhage, as indicated by the red blood cell lying outside the lumen. Focal hemorrhages were common in the septa and about venules (Fig. 6). Neutrophilic granulocytes and lymphocytes were present in small numbers in the interstitial tissue.

## DISCUSSION

Pulmonary edema has been produced experimentally by a variety of techniques, including changes in the gas content and

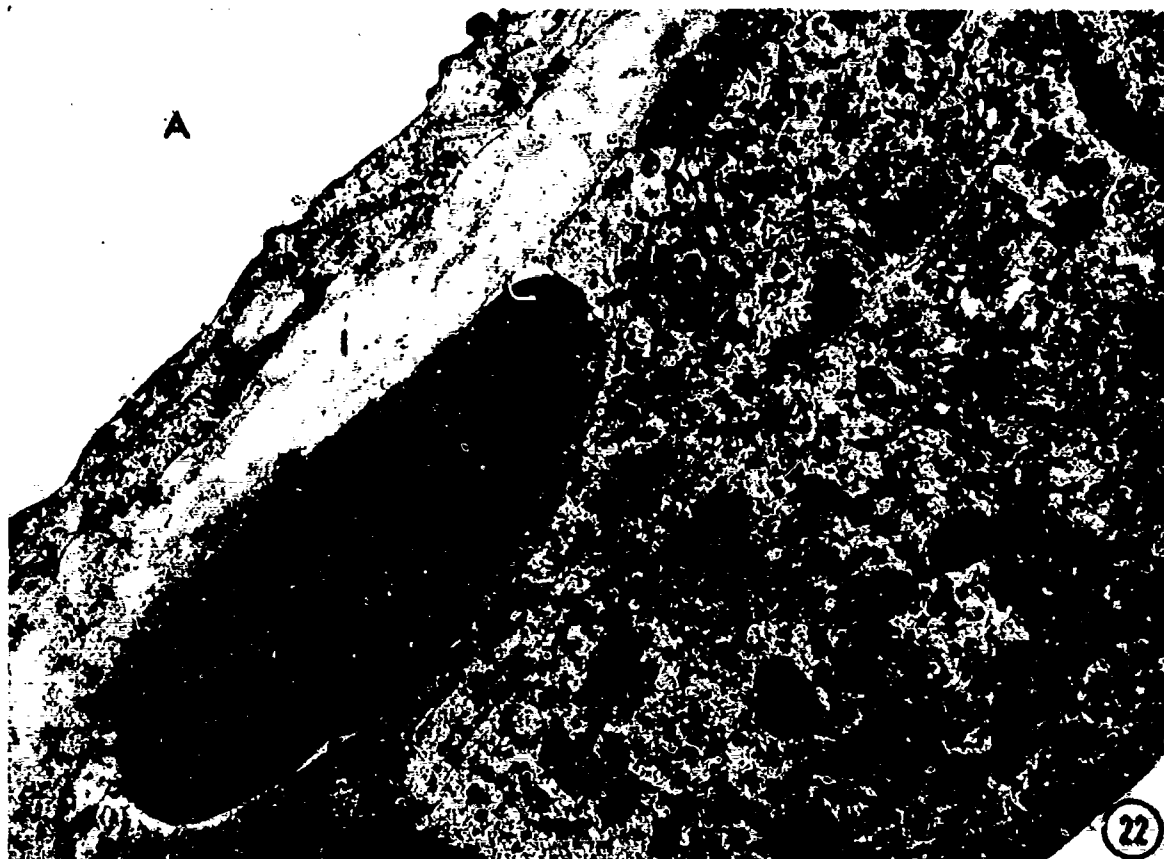


FIG. 22. Emigration of a monocyte. A large monocyte (*M*) fills a septal capillary and protrudes a portion of cytoplasm through a gap between endothelial cells (*arrows*) to reach the basement membrane. A red blood cell lies external to the lumen, although apparently still confined by another endothelial cell process and the basement membrane. Collagen and elastic tissue are tightly bound in the interstitium (*I*). *A*, Alveolar lumen.  $\times 20,000$ .

pressure of inspired air,<sup>10, 17, 26, 29</sup> mechanical obstructions to venous drainage,<sup>10</sup> certain drugs and chemical poisons,<sup>9, 19, 20</sup> and crude bacterial toxins.<sup>1</sup> This report describes the development of interstitial pulmonary edema after a single injection of microgram quantities of a purified bacterial protein, staphylococcal enterotoxin B, in rhesus monkeys. In animals dying of enterotoxemia between 45 and 55 hours after injection, pulmonary edema is the most important pathologic finding. Lungs are from 1.5 to 2.5 times heavier than in control animals. The fluid is predominantly confined to the perivascular and peribronchial interstitial space, and the lymphatics in these areas are engorged. Small foci of alveolar edema are found, as well as occasional mononuclear cell infiltrates of the septa and alveoli.

The ultrastructural basis for this striking

degree of interstitial fluid accumulation appears to be toxic damage of capillary and venule endothelium, which correlates with the observation that intravenously administered, radioactively labeled enterotoxin B accumulates in the lungs of monkeys.<sup>5</sup> A variety of degenerative changes leading to complete necrosis of capillary endothelium has been observed. Some of these changes have been reported previously in experimental pulmonary edema, such as cytoplasmic vacuolation and swelling of rats given  $\alpha$ -naphthylthiourea,<sup>19</sup> Diamox (acetazolamide),<sup>19</sup> or reduced environmental oxygen,<sup>19</sup> and cellular swelling with rarefaction of the cytoplasm in experimental influenza in mice<sup>11</sup> and monocrotaline treatment in rats.<sup>20</sup> Other changes, such as increased electron opacity and granularity of the endothelial cell cytoplasm, have not been reported in pulmo-

nary edema but were described in capillary damage due to a variety of experimental methods.<sup>21, 22</sup> Similarly, the focal endothelial degeneration described in venules after enterotoxin injection has been seen also in allergic inflammation in rabbits.<sup>13, 27</sup>

A very interesting feature of the capillary lesions seen in this and many other studies<sup>4, 6, 7, 13</sup> is the focal nature of the damage, so that injured cells retain continuity with morphologically normal cells and even show varying degrees of damage within a single cell. These observations will have to be explained by any mechanism proposed to account for endothelial cell injury. Another notable feature of the experiment is the delay between the injection of toxin and the onset of edema. Efforts to find histologic and cytologic changes with both light and electron microscopy in lungs of normal weight met with failure. Delays of approximately the same time, 48 to 72 hours in rats<sup>29</sup> and 55 hours in dogs,<sup>26</sup> were reported for the production of pulmonary edema by increasing oxygen tension in the inspired air.

Presumably, the passage of fluid from the bloodstream to the interstitial space is facilitated by the destruction of capillary endothelial cells, a point that might be proved by the use of tracers. Once the fluid has reached the extravascular space, it produces significant secondary capillary and alveolar epithelial lesions. The fluid accumulates predominantly in the adventitia of veins and venules and the contiguous connective tissue. Alveolar walls are not significantly thickened and the collagenous and elastic tissue of the septa are not noticeably spread apart by fluid. However, many alveolar capillaries display herniation of the thin segments of endothelial cells into the vessel lumen because of the accumulation of fluid between the plasma membrane and the basement membrane. A similar phenomenon affects the type I alveolar epithelial cell, which protrudes into the alveolar space. In both sites, some of the blebs contain cellular debris, suggesting that some damage to the cell has occurred. In other examples, however, the cells are clearly undamaged, although strikingly thinned.

Endothelial blebs have been described in several reports. They are found in pulmonary capillaries of rats dying of anthrax toxin,<sup>1</sup> in rats drowned in hypertonic saline,<sup>16</sup> and in normal rat lungs fixed in phosphate-buffered osmium tetroxide.<sup>24</sup> Schulz<sup>19</sup> described them in rats given  $\alpha$ -naphthylthiourea and claimed that they arose from the enlargement of intracellular vacuoles with rupture of a membrane-bound bleb into the vessel lumen. He also saw swelling of the basement membrane in this form of pulmonary edema, and stated that mechanically induced congestive edema and increased  $\text{CO}_2$  in the inspired air also give the same changes. In Kisch's report<sup>9</sup> of "blisters" in the endothelium and epithelium of rabbits given epinephrine, the origin of fluid in the bleb is also unclear. The author, as does Schulz, suggests an intracellular accumulation, yet the photographs may represent an extracellular pressure phenomenon as described above.

The lesions observed in this study may have several deleterious effects on pulmonary physiology: (1) Primary injury to the capillary endothelium, in addition to promoting edema of the interstitium, could directly interfere with the exchange of gases between alveoli and the circulation. (2) The herniation of undamaged endothelial cells into the lumen of capillaries may obstruct blood flow in such areas, with loss of functioning parenchyma. (3) Interstitial perivascular edema has been shown to elevate intrapulmonary venous pressure,<sup>31</sup> further impeding the circulation. (4) Protrusion of alveolar epithelial cells into the airspace and gaps between epithelial cells may interrupt the normally continuous layer of surfactant that lines alveoli. Thereby, the effectiveness of that material in lowering alveolar surface tension would be reduced, and focal collapse promoted.<sup>17</sup> (5) The exudation of fibrin through epithelial cell defects into alveoli may also impair the activity of surfactant by an interaction with the lipoprotein.<sup>25</sup> This would have the same consequences of alveolar collapse and reduction of the surface available for ventilation and gas exchange.

## SUMMARY

Interstitial pulmonary edema was produced in rhesus monkeys by intravenous injections of staphylococcal enterotoxin B, a purified protein toxin. The primary pathologic change, as revealed by electron microscopy, was capillary endothelial cell degeneration and necrosis, with less frequent damage to the endothelium of venules. Secondary phenomena were interstitial hemorrhage and edema and a histiocytic infiltrate. There was striking herniation of capillary endothelium into the vascular lumen which may contribute significantly to decreased pulmonary perfusion in this toxemia.

**Acknowledgments.** The author wishes to express his appreciation to Dr. John D. White for training and encouragement in the use of the electron microscope and other techniques, and to Mrs. Frances G. Shirey for her expert technical assistance.

## REFERENCES

1. Beall, F. A., and Dalldorf, F. G. The pathogenesis of the lethal effect of anthrax toxin in the rat. *J. Infect. Dis.* 116: 377, 1966.
2. Bertalanffy, F. D. On the nomenclature of the cellular elements in respiratory tissue. *Amer. Rev. Resp. Dis.* 91: 605, 1965.
3. Cohn, Z. A. The metabolism and physiology of the mononuclear phagocytes. In *The Inflammatory Process*, edited by Zweifach, B. W., Grant, L., and McCluskey, R. T., p. 323. New York, Academic Press, Inc., 1965.
4. Cotran, R. S. The delayed and prolonged vascular leakage in inflammation. II. An electron microscopic study of the vascular response after thermal injury. *Amer. J. Path.* 46: 589, 1965.
5. Crawley, G. J., Gray, L., Leblang, W. A., and Blanchard, J. W. Bloodbinding, distribution and excretion of staphylococcal enterotoxin in monkeys. *J. Infect. Dis.* 116: 48, 1966.
6. Friederici, H. H., and Pirani, C. L. The fine structure of peripheral capillaries in experimental nephrotic edema. *Lab. Invest.* 13: 250, 1964.
7. Ham, K. N., and Hurley, J. V. Acute inflammation: an electron microscope study of turpentine-induced pleurisy in the rat. *J. Path. Bact.* 90: 365, 1965.
8. Kent, T. H. Staphylococcal enterotoxin gastroenteritis in rhesus monkeys. *Amer. J. Path.* 48: 387, 1966.
9. Kisch, B. Electron microscopy of the lungs in acute pulmonary edema. *Exp. Med. Surg.* 16: 17, 1958.
10. Kisch, B. Electron microscopy of capillary hemorrhage. I. Post hypoxemia hemorrhage in the lungs. *Exp. Med. Surg.* 23: 117, 1965.
11. Lamanna, C. Immunological aspects of airborne infection: some general considerations of response to inhalation of toxins. *Bact. Rev.* 25: 323, 1961.
12. McKay, D. G. *Disseminated Intravascular Coagulation*, p. 10. New York, Hoeber Medical Division, Harper and Row, Publishers, 1965.
13. Movat, H. Z., and Fernando, N. V. P. Acute inflammation. The earliest fine structural changes at the blood-tissue barrier. *Lab. Invest.* 12: 895, 1963.
14. Plummer, M. J., and Stone, R. S. The pathogenesis of viral influenzal pneumonia in mice. *Amer. J. Path.* 45: 95, 1964.
15. Rapoport, M. I., Hodoval, L. F., Grogan, E. W., McGann, V., and Beisel, W. R. The influence of specific antibody on the disappearance of staphylococcal enterotoxin B from the blood. *J. Clin. Invest.* 45: 1365, 1966.
16. Reidbord, R. E., and Spitz, W. U. Ultrastructural alterations in rat lungs. Changes after intratracheal perfusion with fresh water and seawater. *Arch. Path. (Chicago)* 81: 103, 1966.
17. Schaeffer, K. E., Avery, M. E., and Bensch, K. Time course of changes in surface tension and morphology of alveolar epithelial cells in CO<sub>2</sub>-induced hyaline membrane disease. *J. Clin. Invest.* 43: 2080, 1964.
18. Schantz, E. J., Roessler, W. G., Wagman, J., Spero, L., Dummery, D. A., and Bergdoll, M. S. Purification of staphylococcal enterotoxin B. *Biochemistry (Wash.)* 4: 1011, 1965.
19. Schulz, H. *The Submicroscopic Anatomy and Pathology of the Lung*, p. 88. Berlin, Springer-Verlag, 1959.
20. Sonnad, J., Valdivia, E., and Hayashi, Y. Electron microscopy of the early pulmonary lesions produced by monocrotaline. Presented to the American Association of Pathologists and Bacteriologists, March 1966.
21. Sprinz, H. Cholera: pathology in man and experimental animals. In *Cholera, Combined Clinical Staff Conference at the National Institutes of Health*, Gordon, R. S., Jr., Moderator. *Ann. Intern. Med.* 64: 1328, 1966.
22. Steiner, J. W., Carruthers, J. S., and Kalifat, S. R. Vascular alterations in the liver of rats with extrahepatic biliary obstruction. *Exp. Molec. Path.* 1: 427, 1962.
23. Sugiyama, H., Chow, K. L., and Dragstedt, L. R. Study of emetic receptor sites for staphylococcal enterotoxin in monkeys. *Proc. Soc. Exp. Biol. Med.* 108: 92, 1961.

24. Takahashi, K., Kawano, A., Ota, O., and Otsuka, S. Electron microscopic studies on the lung tissue. *Tokushima J. Exp. Med.* 8: 149, 1961.
25. Taylor, F. B., Jr., and Abrams, M. E. Effect of surface active lipoprotein on clotting and fibrinolysis, and of fibrinogen on surface tension of surface active lipoprotein. With a hypothesis on the pathogenesis of pulmonary atelectasis and hyaline membrane in respiratory syndrome of the newborn. *Amer. J. Med.* 40: 346, 1966.
26. Totten, R. S., Cauna, D., Cimon, I. M., Pautler, S., and Safar, P. The toxic effects of high oxygen concentration on dog lung: pathogenetic considerations. Presented to the International Academy of Pathology, March 1966.
27. Urichara, T., and Movat, H. Z. Allergic inflammation. IV. The vascular changes during the development and progression of the direct active and passive Arthus reactions. *Lab. Invest.* 13: 1057, 1964.
28. Weed, L., Michael, A. C., and Harger, R. N. Fatal staphylococcus intoxication from goat milk. *Amer. J. Public Health* 33: 1314, 1943.
29. Weibel, E. R. Conducting airways and respiratory surface. Presented to the International Academy of Pathology, March 1966.
30. Weibel, E. R., and Palade, G. E. New cytoplasmic components in arterial endothelia. *J. Cell Biol.* 33: 101, 1964.
31. West, J. B. Perivascular edema, a factor in pulmonary vascular resistance. *Amer. Heart J.* 70: 570, 1965.